Electrical, optical and structural characterization of high-*k* dielectric ZrO$_2$ thin films deposited by the pyrosol technique

G. REYNA-GARCÍA
UAM-I, Iztapalapa 09340, México DF, México

M. GARCÍA-HIPÓLITO, J. GUZMÁN-MENDOZA
IIM, UNAM, Coyacan 04510, México DF, México

M. AGUILAR-FRUTIS
CICATA-IPN, Miguel Hidalgo 11500, México, DF, México

C. FALCONY
CINVESTAV-IPN, Apdo. Postal 14-740, 07000, México DF, México

High-*k* dielectric zirconium oxide (ZrO$_2$) thin films have been deposited on silicon substrates at temperatures from 400 to 600 °C using the spray pyrolysis technique. The films were deposited from two spraying solution concentrations (0.033 and 0.066 M) of zirconium acetylacetonate dissolved in N,N-dimethylformamide. These films were stoichiometric, transparent and with a very low surface roughness (5–40 Å). The refractive index of these films was of the order of that obtained for a bulk material (2.12). Films deposited with high molar concentration presented the best electrical characteristic, have a dielectric constant in the range 12.5–17.5, depending on the deposition temperature, and can stand electric fields up to 3 MV cm^{-1} without observing destructive dielectric breakdown. Transmission electron microscopy measurements, indicate that the films consist of nano-crystallites of the tetragonal ZrO$_2$ crystalline phase embedded into an amorphous matrix. Infrared spectroscopy measurements of the films show peaks associated with ZrO$_2$ and a peak related to silicon dioxide (SiO$_2$). The analysis of spectroscopic ellipsometry measurements on these films indicates the existence of a layer at the ZrO$_2$/Si interface composed of SiO$_2$ as well as ZrO$_2$ and crystalline silicon.
© *2004 Kluwer Academic Publishers*

1. Introduction

High dielectric constant (high-*k*) materials are currently investigated for the replacement of SiO$_2$ as gate insulator in advanced metal-oxide-semiconductor (MOS) field effect transistors [1]. It is required that high-*k* dielectric gate stacks withstand the high-temperatures (≈ 1000 °C) involved in the transistor fabrication processes. Metal oxides such as Al$_2$O$_3$, Y$_2$O$_3$, La$_2$O$_3$, ZrO$_2$, and HfO$_2$ are good candidates for this purpose because they are thermally stable on Si even at these high temperatures [2]. ZrO$_2$ has a high dielectric constant (in the range 14–25), and a reasonable barrier height (2 eV) when deposited on Si [3]. In addition, ZrO$_2$ has attracted much attention in science and technology because of its high melting temperature, refractive index, and hardness, as well as low thermal conductivity and corrosion barrier properties [4]. Because of these properties, ZrO$_2$ has been studied in connection with applications such as optical coatings [5], insulating layers in very large scale integrated circuits [6], buffer layers for high-T_c oxide superconductors [7] and as active layers in electro-

luminescent flat panel displays [8]. ZrO$_2$ layers have been deposited by physical and chemical vapor deposition processes (PVD, CVD), atomic layer deposition (ALD), remote plasma enhanced chemical vapor deposition (RPECVD) [9–12], among other techniques. High quality ZrO$_2$ thin films deposited by CVD have been reported by Balog *et al.* [13] with a dielectric constant in the range 17–18 and flatband voltage shifts ranging from −600 to +200 mV. Shappir *et al.* [14] studied ZrO$_2$ thin films deposited by metalorganic CVD at 450 °C, the dielectric constant obtained in these films was in the range 14–19 (in this case, *k* decreased with increasing annealing temperature). Also spray pyrolysis has been used to obtain homogeneous ZrO$_2$ thin films from alcohol solutions of zirconium acetylacetonate, followed by a postdeposition annealing process in flowing oxygen [15]. The spray pyrolysis technique is a simple and low cost deposition process that is compatible with large area applications. In the present work, high quality zirconium oxide thin films have been obtained by spray pyrolysis deposition using two different molar

concentration solutions (0.033 and 0.066 M) of zirconium acetylacetonate ($Zr(acac)_4$) dissolved in N,N-Dimethylformamide, (N,N-DMF). No post deposition annealing treatments were performed on these films. The optical structural and electrical characteristics of these films are reported. Transmission electron microscopy (TEM) observations indicate that these films have small crystallites immersed in a predominant amorphous phase.

2. Experimental details

The spray pyrolysis technique has been described previously [16, 17]. For this work, the deposition apparatus consisted of an ultrasonic generator, operated at 0.8 MHz, for mist production from an aqueous solution. The mist is transported to the surface of the substrate by means of a carrier gas. The substrate was placed on top of a molten tin bath, (used as heating system) in order to achieve the pyrolysis reaction. Two molar concentrations (0.033 and 0.066 M) of $Zr(acac)_4$, from Aldrich Inc. Co., dissolved in N,N-DMF, from Mallinckrodt were used as spraying solutions. Air was used as carrier gas at a flow rate of approximately 14 l min^{-1}. The films were deposited at substrate temperatures in the range 400–600 °C on n-type silicon substrates of high resistivity (200–300 Ω cm), for IR measurements, and on n-type Si of low resistivity (0.1–10 Ω cm), for the electrical measurements, and on quartz slides. The quartz substrates were used for optical absorption measurements in the 200–900 nm range. These measurements were performed with a commercial ultraviolet-visible (UV–Vis) spectrophotometer. The thickness and refractive index of the films were measured with a manual ellipsometer at 633 nm. A Jobin–Yvon phase modulated spectroscopic ellipsometer (UVISEL model), operating in an energy range 1.5–4.75 eV, was also used to obtain the optical properties of the films. The ellipsometer is operated with the Elli41 software that performs a χ^2 minimization process, through a regression analysis of the parameters involved according to a proposed model. The surface roughness measurements were carried out on a Park Scientific Instruments Atomic Force Microscope (AFM). A scanning electron microscope (JEOL, JSM-6300), equipped with the Voyager microanalysis system from Noran Instruments, was used to obtain the chemical analysis by Energy Dispersive Spectroscopy (EDS). TEM analysis was carried out on a JEOL 2010 EM, operated at 200 kV. Before observing the films in the TEM, a sample preparation procedure was carried out. The procedure involved thinning the silicon substrate, first, until it reached 100 µm in thickness, using a TEM Specimen Disk Grinder (model 623) and a 500 grid silicon carbide sandpaper. A further thinning was achieved with a Precision Dimple Grinder (model 656/3), from Gatan, using alumina (0.05 µm) suspensions to form a semi-spherical cavity, leaving a sample thickness of approximately 40 µm, and, finally, a Precision Ion Polish System, also from Gatan, was used to get the final thinning of the samples, this was used at an inclination angle of 3°. A 750 Magna-IR NICOLET spectrometer was used for IR measurements. The current versus voltage and capacitance versus voltage measure-

ments were carried out in a commercial equipment by Keithley instruments. For these electrical measurements, the films deposited on low-resistance silicon substrates, were integrated in MOS structures, by thermally evaporating aluminum contacts on top of the films defining an area of 0.011 cm^2.

3. Experimental results

Fig. 1 shows the deposition rate of the films as a function of the inverse of the substrate temperature during deposition for the two spraying solution molarities used. The deposition rate is much lower for films deposited with 0.033 M, (lower than 7.5 Å/s). The total thickness of the films was about 1000 Å. It is also observed that the deposition rate is almost independent of the substrate temperature for temperatures above 500 °C. An activation energy, calculated for temperatures up to 500 °C, of about 14.55 kJ/mol was obtained for low molarity films, in contrast, an activation energy of 42.86 kJ/mol was obtained for films deposited with 0.066 M, in the same range of temperatures. Fig. 2 shows the %Transmission curve as a function of light energy in the UV–Vis range for a film deposited at 500 °C and 0.066 M. It is observed an 80% transmission in the visible for this film. In all cases the films resulted transparent in the visible energy range, showing an absorption edge corresponding to an average value for the optical bandgap of 5.8 eV. The inset of this figure shows the behavior of the films refraction index at 630 nm as a function of deposition temperature. The maximum refractive index value obtained was 2.12, and corresponds to a film deposited at 550 °C and a molar concentration of 0.066 M. Natural bulk zirconium oxide (baddeleyite) has a refractive index in the range from 2.13 to 2.20 (in monoclinic phase) [18].

Fig. 3 shows a typical surface morphology observed on the ZrO_2 films studied, as determined by AFM. In general, the surface roughness of the films is very low. The surface roughness for the films deposited with the 0.066 M solution is lower than 10 Å, but the surface roughness of the films deposited with the 0.033 M
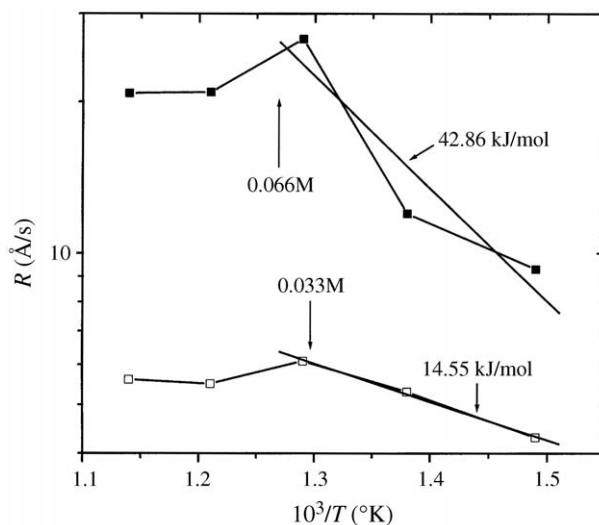

Figure 1 Deposition rate of the zirconium oxide films as a function of $10^3/T$. The figure shows the activation energies of the films deposited with the different molar concentrations.
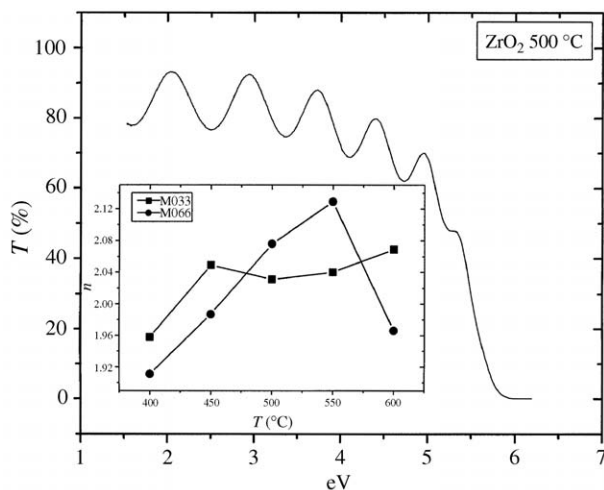
Figure 2 Typical transmission spectrum for a zirconium oxide film deposited at 500 °C with a molar concentration of 0.066 M. The inset shows the behavior of the refractive index of the films, deposited with molar concentrations of 0.033 and 0.066 M, measured at 633 nm, as a function of the substrate temperature.
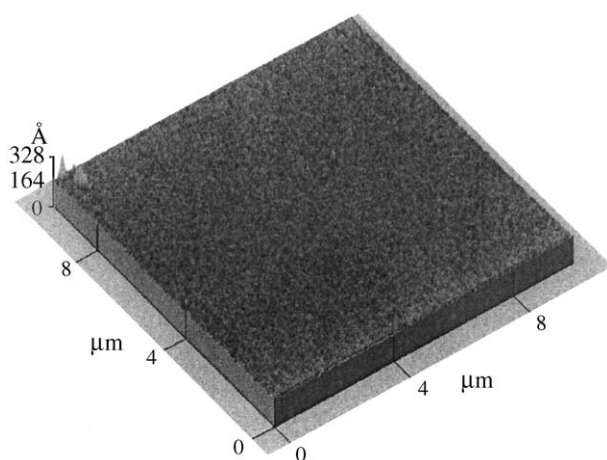

Figure 3 Surface morphology of a zirconium oxide thin film, as derminated by AFM, for a film deposited on silicon substrate at 500 °C and with a molar concentration of 0.033 M.

solution reaches values up to 40 Å. A series of infrared spectra is shown in Fig. 4 for the ZrO_2 films. A band associated with ZrO_2 is clearly observed at $420 \, cm^{-1}$, other small peaks, located approximately at 500 and $660 \, cm^{-1}$, associated to ZrO_2, can also be seen. The infrared absorption bands reported for zirconium oxide are located close to 725, 660, 580, 500, and $420 \, cm^{-1}$ [19]. The presence of –OH stretching bonds (around 3400–$3600 \, cm^{-1}$) is observed for films deposited at 400, 450 and 500 °C. However, for deposition temperatures

above 500 °C, the presence of these –OH related bonds was reduced. The infrared spectra show in addition a band centered between 1000 and $1100 \, cm^{-1}$, due to the formation of SiO_2 at the interface of the silicon substrate. The formation of SiO_2 probably occurs during the deposition process of the film, since the substrate is exposed to air-ambient conditions. The intensity of the SiO_2 IR band is more noticeable for higher deposition temperatures (600 °C).

The polycrystalline nature of the films was studied in TEM. For this purpose, samples deposited at 500 and 600 °C and molar concentrations of 0.033 M, and 0.66 M were prepared (as explained in the previous section) and observed in plan view mode (normal to the film surface) in the TEM. Fig. 5 shows the TEM micrographs for (a) a film deposited at 600 °C, with a molar concentration of 0.033 M, (b) a film deposited at 600 °C and a molar concentration of 0.066 M, (c) a high resolution micrograph obtained for a film deposited at 500 °C and a molar concentration 0.033 M, and (d) an electron diffraction pattern for the film shown in Fig. 5(a). The presence of very small crystalline features is observed in all cases, but the size of the crystallites is larger for the films deposited at higher molar concentrations. The electron diffraction pattern shows concentric rings, indicating the polycrystalline nature of the films. The indexed rings of the diffraction pattern correlate with the tetragonal phase of zirconia. Similar characteristics are observed for the other films studied. The chemical composition of the films as a function of the substrate temperature determined by EDS is shown in Fig. 6. From this plot it is observed that the atomic ratio of oxygen to zirconium is close to 2.0, but tends to decrease as the substrate temperature is increased. Stoichiometric films are obtained up to a substrate temperature of 550 °C, approximately. The presence of carbon in the films was also evident. However, the precise amount of carbon found has not been determined yet. This carbon presence is most likely associated with the organic reagents used for the film deposition process.

The inset in Fig. 7 shows a high frequency capacitance versus voltage curve for a MOS structure incorporating a ZrO_2 film deposited at 500 °C with a molar concentration of 0.066 M. From the capacitance curve in the accumulation region, the dielectric constant of the films was determined and is shown as a function of the substrate temperature in Fig. 7. It is observed that the dielectric constant varies in the range 12.5–17.5, approximately, (the dielectric constant has a minimum around 500 °C). Table I summarizes the dielectric characteristics (*I–V* and *C–V* measurements) of the

T A B L E I Dielectric characteristcs of the films of zirconium oxide deposited with a molar solution of 0.066 M and substrate temperatures from 450 to 650 °C

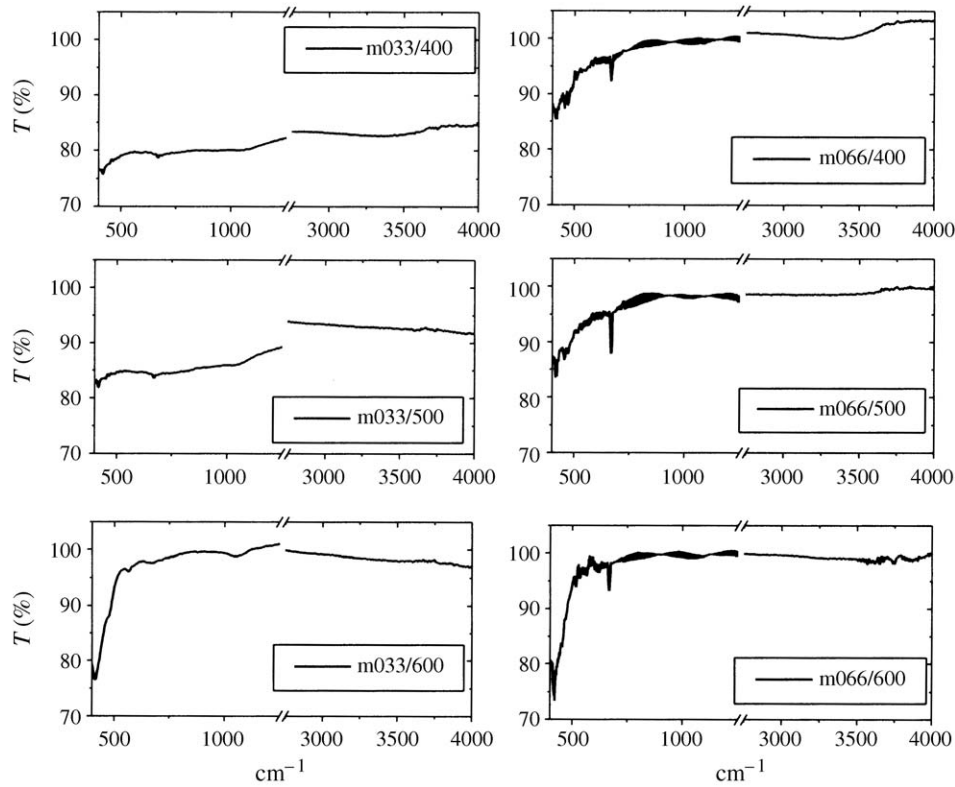|	Dielectric characteristics (0.066 M films)			
Substrate temperature	Average ΔVFB (V)	Average current ($\times 10^{-4}$ amp)	Average electric field (MV/cm)	Dielectric constant
450	− 0.810	9.7	0.49 ± 0.23	17.5
500	+ 3.19	4.2	1.04 ± 0.54	12.5
550	− 0.702	8.5	0.49 ± 0.05	13.8
600	− 0.775 to + 2.53	5.3	0.89 ± 0.51	14.1

441

Figure 4 Infrared spectroscopy spectra of the zirconium oxide films deposited at 400, 500 and 600 °C, with the molar concentrations of 0.033 and 0.066 M.

films obtained when they are deposited with a molar concentration of 0.066 M. The best results were obtained for substrate temperatures above 450 °C. Films deposited with a molar concentration of 0.033 M showed poor dielectric characteristics in general and are not listed in Table I. The average electric field applied to the different films and its average leakage current density observed, as well as the dielectric constant are also shown in Table I. Fig. 8 shows the best ramp *I–V* obtained for a capacitor fabricated with a film deposited at 500 °C with a molar concentration solution of 0.066 M. It is observed that an electric field in the range of 2 to 3 MV cm^{-1} can be applied without observing destructive dielectric breakdown. Spectroscopic ellipsometry results are illustrated in Fig. 9, where the experimental and theoretical curves for the ellipsometric angles; Psi and Delta, (Ψ, Δ), as a function of photon energy, are shown for a sample deposited at 500 °C and with the 0.066 M solution. The theoretical curve that fits the experimental data was obtained assuming a three layer model (the best model found). The explanation for this model is as follows; the first layer (considered as a roughness layer) of the model consisted of a mixture of crystalline silicon (c-Si), zirconium oxide (ZrO$_2$-disp), and silicon dioxide (SiO$_2$-disp). The volume fraction of these phases were considered fixed in; 33, 33 and 34%, respectively. Both SiO$_2$-disp and ZrO$_2$-disp were built through Sellmeier transparent dispersion functions. The Sellmeier dispersion function is given by the relation; $n^2 = A + B\left[\lambda^2/(\lambda^2 - \lambda_0^2)\right]$ [20], where *n* and λ are the refractive index and wavelength of light, respectively. This relation involves three parameters to be fitted; *A*, *B* and λ_0. In particular, to find the SiO$_2$ dispersion function

parameters (SiO$_2$-disp), the following experiment was done; a bare Si substrate was placed on top of the molten tin used to deposit the films. The Si substrate was kept there for one minute, approximately, at temperatures in the range 400–600 °C. The grown film (of silicon dioxide) was then spectroscopic ellipsometry modeled. In order to not consider too many parameters, *A* the parameter of the model was considered fixed to 1. The best *B* and λ_0 values, obtained through the χ^2 minimization process, were; 0.978 and 225.08 nm, respectively. Then, the parameters found for SiO$_2$-disp were then considered fixed when modeling the first layer of the model applied to the films deposited. For zirconium oxide (ZrO$_2$-disp), the *B* and λ_0 parameters were let to vary during the χ^2 minimization, but *A* parameter was also fixed to 1. In summary, the dispersion functions built for silicon dioxide as well as for zirconium oxide (SiO$_2$ and ZrO$_2$-disp) were used to fit first layer of the model proposed to the acquired experimental spectroscopic ellipsometry data of the films, using the Bruggeman Effective Medium Approximation (BEMA) [4]. The BEMA assumes that the individual components that form the part of a medium are physically much smaller than the wavelength of light, and can be used therefore to simulate microroughness. The second layer of the model, considered as the main layer, consisted of 100 vol % fraction of ZrO$_2$-disp. Finally, the third layer consisted of a mixture of Voids and ZrO$_2$-disp, in fixed volume, fractions of 50%, respectively, and using also Bruggeman Approximation. This layer is also considered as a roughness layer. The optical properties of voids were obtained from the data bank of the Elli41 software
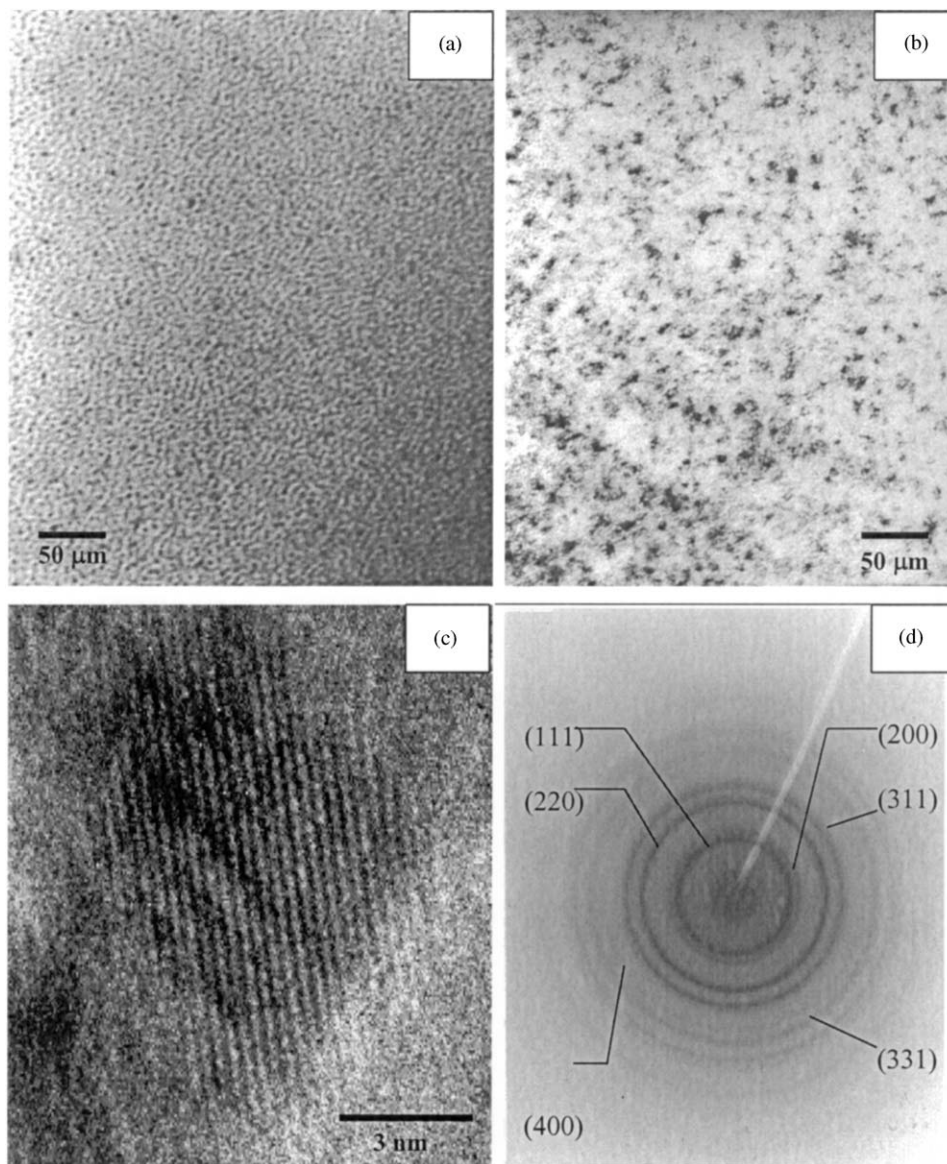
442

Figure 5 TEM microscopy images of ZrO$_2$ thin films. (a) Film deposited at 600 °C with a molar concentration of 0.033 M. (b) Film deposited at 600 °C with a molar concentration of 0.066 M. (c) High resolution micrograph for a film deposited at 500 °C with a molar concentration of 0.033 M. (d) Indexed electron diffraction pattern for the film shown in (a).

spectroscopic ellipsometer. Only the film deposited at 600 °C and with the 0.066 M, fitted better with a 50 vol % fraction of SiO$_2$-disp and a 50 vol % fraction of ZrO$_2$-disp, in the first (roughness) layer. In the model described, the parameters that were fitted through the χ^2 minimization process of the parameters involved were: (a) Thickness of layer 1, (b) Thickness of layer 2, (c) Thickness of layer 3, (d) B of layer 2, and (e) λ_0 of layer 2. The best fitted results are summarized in Table II for each sample deposited at the different substrate temperatures. In all of these results a variation in the thickness of layer 1 can be observed. The thickness of the layer 2 results in a much more homogeneous variation in general, and it ranges from 640 to 1060 Å, approximately. The thicknesses of layer 3 result thicker for films deposited with 0.033 M than for films deposited with 0.066 M. The last row in Table II gives the χ_2 minimization value of the fittings. A good agreement between the experimental data and the best model proposed is obtained in most cases, as is illustrated graphically in Fig. 9.

4. Discussion

The growth rate of the films in Fig. 1 shows an exponential behavior as a function of $10^3/T$, for both types of molarities used and up to a substrate temperature of 500 °C. Above 500 °C the growth rate remains almost constant. This behavior might indicate that the growth rate for temperatures above 500 °C is mainly controlled by the diffusion of reactants to the reacting surface. Since a higher concentration of reactants is supplied in the solution prepared with a molar concentration of 0.066 M, a higher growth rate is observed as expected. This deposition rate regime is similar to the ones shown in several films deposited by a CVD process [21]. In addition, the activation energies found are in the range observed when dielectric films are deposited by the pyrosol technique [22]. The refractive index of the films, inset of Fig. 2, is in all cases lower than the value reported for bulk zirconia. The highest value (2.12) obtained in our case (close to the reported value of bulk zirconia), corresponds to a film deposited at a substrate temperature of 550 °C and a molar concentration
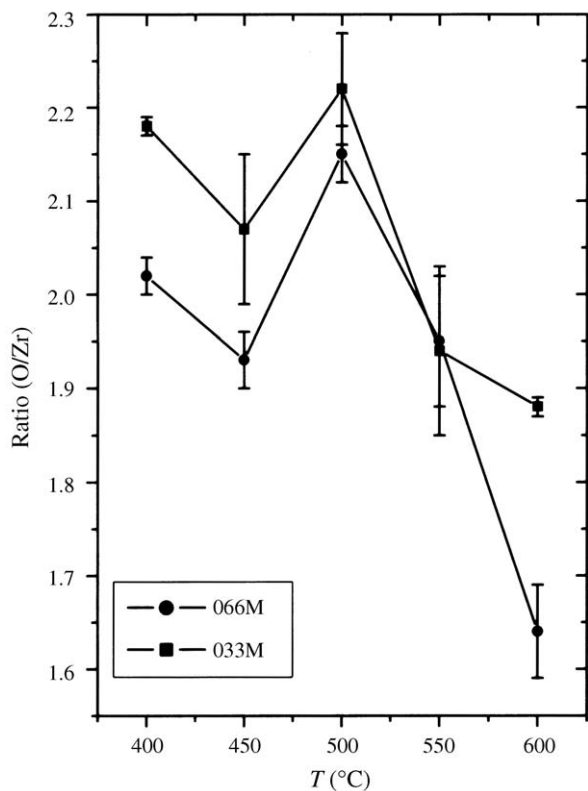
443

Figure 6 Chemical composition of the zirconium oxide films as determined by EDS. The graph shows the ratio of at% oxygen to at% zirconium as a function of the substrate temperature.

Figure 8 Ramp *I–V* for a capacitor fabricated with a thin film of zirconium oxide deposited at 500 °C and with a molar concentration of 0.066 M.

0.066 M solution. These films show a clear polycrystalline nature (see Fig. 5). Even though X-ray diffraction measurements were performed with a powder diffraction
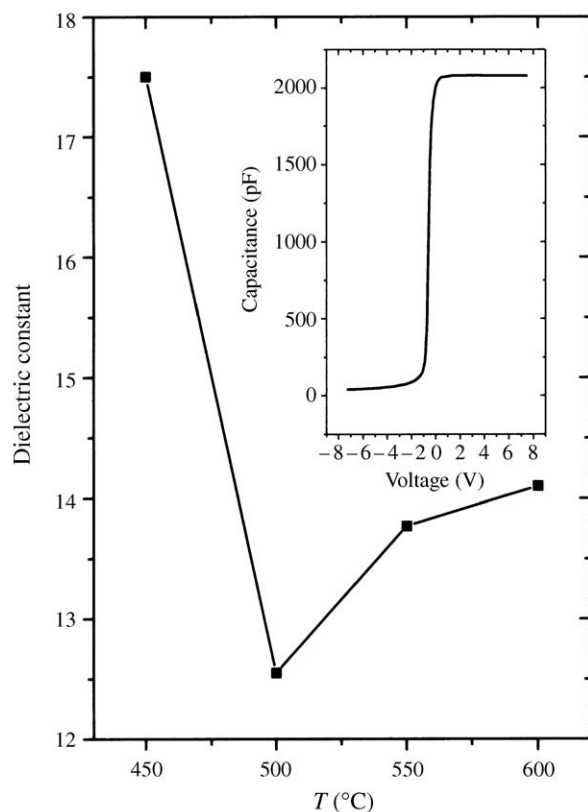

Figure 7 Capacitance versus Voltage curve for a film of zirconium oxide deposited at 450 °C. The inset shows the dielectric constant of the films as a function of the substrate temperature. The films were deposited with a molar concentration of 0.066 M.
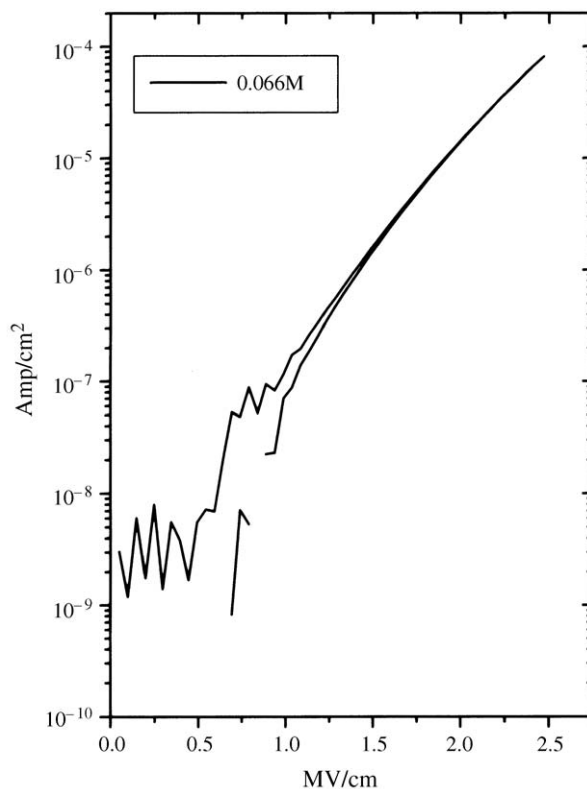
equipment on these films (not shown here) it was only through electron diffraction that the tetragonal phase of zirconia was observed. Probably the small size of the crystalline features observed in TEM images is not enough to be observed with the X-ray diffraction equipment. Infrared spectroscopy measurements also show the existence of SiO_2 in the films. The band observed between 1000 and 1100 cm^{-1} corresponds to the stretching band of Si–O [23]. From the experiments carried out we can state that silicon oxide is formed probably during deposition of the films of ZrO_2, this is mainly due to the fact that the substrate is exposed to air from the ambient during the deposition process. The trend shown by the ratio of oxygen to zirconium in at%, determined by EDS, suggests that the films are not fully oxidized when they are deposited at a substrate temperature of 600 °C. This could be associated with oxygen de-adsorption occurring during the deposition process at high temperatures [24]. From spectroscopic ellipsometry results, the best fittings (minimum χ^2 values) between the experimental data and the theoretical curve were obtained when the model includes a first roughness layer composed from silicon dioxide, zirconium dioxide and in most cases crystalline silicon. It has been discussed by other authors that the system $(ZrO_2)_x$–$(SiO_2)_{1-x}$ is a very encouraging one, since this system combines the desirable properties of the two different oxides. The effect of adding SiO_2 to ZrO_2 produces an amorphous film that is thermodynamically stable on silicon (for low leakage currents) [25]. In this respect, it is thought that the approach of using the BEMA to describe the interface of the films deposited on silicon was very important. The same approximation was used by Hu and Tay [4]. Since the dielectric properties of the
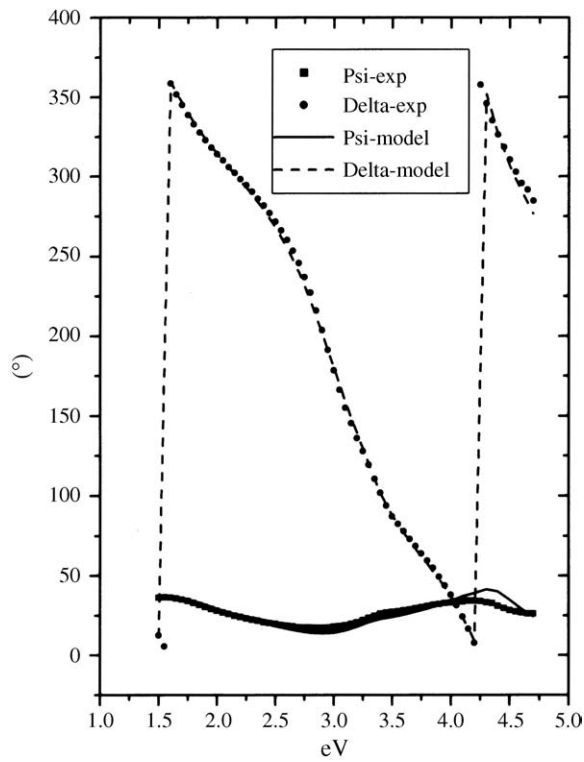
Figure 9 Experimental and theoretical spectroscopic ellipsometry angles Psi and Delta (Ψ, Δ) for a thin film deposited at 500 °C and with a molar concentration of 0.066 M.

films depend strongly on film composition, density and structure [23], it is thought that the role of the roughness layer, immediately on top of the silicon substrate (layer 1 of Table II), might play a very important role in the determination of the dielectric characteristics of the films. The dielectric constant of the films (12.5–17.5), was found lower or close to that of pure bulk zirconium oxide (20–25 or 14–25 [3, 14]). This is probably due to the influence of the SiO_2 component found in the roughness layer, since it could behave as a capacitance stack and in this case, it will result in a reduction of the effective dielectric constant measured. The behavior of this interface layer thickness with deposition temperature does not have a simple monotonic correlation as expected. The reason for this behavior is not clear at the moment and further work is required to fully understand this aspect. In addition, it is found that the films deposited with 0.066 M are more dense than the films deposited with a molar concentration solution of 0.033 M (this can be inferred from the inset of Fig. 2, through the refractive index curve). The surface roughness, determined by AFM, is also lower for films deposited with a molar concentration solution of 0.066 M. This result is also confirmed by spectroscopic ellipsometry (see Table II, layer 3). The overall results show that the films deposited with a molar concentration solution of 0.066 M have much better characteristics, and

T A B L E I I Spectroscopic ellipsometry results of the films of zirconium oxide deposited with molarities of 0.033 and 0.066 M at substrates temperatures from 400 to 600 °C

	ZrO₂ (Spectroscopic ellipsometry results)									
	0.033 M					0.066 M				
T (°C)	400	450	500	550	600	400	450	500	550	600*
Layer 1 Thickness (Å) 33% Silicon-db +33% ZrO₂-disp +34% SiO₂-disp	—	74.7 ± 8.4	52.1 ± 15.3	10.4 ± 9.5	18.8 ± 9.9	61.6 ± 11.3	46.6 ± 10.1	148.2 ± 6.1	90.6 ± 11.8	127.3 ± 58.6
*50% SiO₂-disp + 50% ZrO₂-disp										
Layer 2 Thickness (Å) ZrO₂-disp	769.9 ± 12.1	789.6 ± 20.2	725.8 ± 22.4	838.5 ± 21.5	857.5 ± 25.5	1060.1 ± 35.9	814.5 ± 29.4	911.3 ± 27.4	702.3 ± 24.1	638.6 ± 68.4
Layer 3 Thickness (Å) 50% ZrO₂-disp +50% voids-db	85.1 ± 21.2	24.0 ± 10.7	97.6 ± 27.7	108.8 ± 28.3	37.4 ± 18.8	0.5 ± 2.5	1.8 ± 4.8	18.0 ± 14.6	44.5 ± 15.6	53.3 ± 19.1
ZrO₂ Sellmeier-parameters and fitting										
A	1.000 ± 0.766	1.000 ± 1.285	1.000 ± 1.809	1.000 ± 1.216	1.000 ± 1.391	1.000 ± 1.358	1.000 ± 2.051	1.000 ± 1.105	1.000 ± 1.215	1.000 ± 1.112
B	2.508 ± 0.759	3.000 ± 1.268	3.000 ± 1.800	2.551 ± 1.203	3.000 ± 1.340	2.492 ± 1.393	3.092 ± 2.041	3.196 ± 1.105	3.581 ± 1.221	2.732 ± 1.101
λ_0	136.188 ± 14.374	142.508 ± 21.610	103.717 ± 25.336	122.274 ± 21.994	143.413 ± 22.603	145.105 ± 27.706	148.318 ± 31.679	131.621 ± 17.562	113.867 ± 17.770	131.01 ± 20.233
χ_2	9.61	20.3	20.8	15.10	41.0	43.99	59.2	27.26	26.02	10.78

445

this is probably the reason for their better electrical behavior with respect to the films deposited at lower molarity.

5. Conclusions

Zirconium acetylacetonate was used to obtain high quality zirconium oxide thin films, without any further annealing procedures, by the pyrosol process. The films present dielectric constants in the range 12.5–17.5, depending on the experimental conditions, and can stand electric fields in the range of 2–$3\,\mathrm{MV\,cm^{-1}}$, without observing destructive dielectric breakdown and with relatively small flatband voltage shifts. The chemical composition of the films show that they are stoichiometric when they are deposited at temperatures lower than $550\,^{\circ}\mathrm{C}$. TEM measurements indicate the polycrystalline nature of the films. The as deposited films were transparent, with a very low surface roughness and a refractive index up to 2.12. Spectroscopic ellipsometry modeling results indicate the presence of an interface roughness layer consisting of a mixture of SiO_2, ZrO_2 and crystalline silicon on top of the silicon substrate. This interface layer, as well as the overall optical and structural characteristics of the films are probably responsible for the main dielectric characteristics of the films.

References

1. S. RAMANATHAN, C.-M. PARK and P. MCLNTYRE, *J. Appl. Phys.* **91** (2002) 4521.
2. S. STEMMER, Z. CHEN and R. KEDING, *ibid.* **92** (2002) 82.
3. M. HOUSSA, J. L. AUTRAN, A. STESMANS and M. M. HEYNS, *Appl. Phys. Lett.* **81** (2002) 709.
4. Y.-Z. HU and S.-P. TAY, *J. Vac. Sci. Technol. B* **19** (2001) 1706.
5. A. DUPARRE, E. WELSCH, H. G. WALTER, N. KAISER, H. MUELLER, E. HACKER, H. LAUTH, J. MEYER and P. WEISSBRODT, *Thin Solid Films* **250** (1994) 1.
6. E. T. KIM and S. G. YOON, *ibid.* **227** (1993) 7.
7. X. D. XU, R. E. MUENCHAUSEN, N. S. NOGAR, A. PIQUE, R. EDWARDS, B. WILKENS, T. S. RAVI, D. M. WANG and C. Y. CHEN, *Appl. Phys. Lett.* **58** (1991) 304.
8. M. GARCIA-HIPOLITO, E. MARTINEZ, O. ALVAREZ-FREGOSO, C. FALCONY and M. A. AGUILAR-FRUTIS, *J. Mater. Sci. Lett.* **20** (2001) 1799.
9. M. A. CAMERON and S. M. GEORGE, *Thin Solid Films* **348** (1999) 90.
10. L. NIINISTÖ, M. RITALA and M. LESKELÄ, *Mat. Sci. Eng. B* **41** (1996) 23.
11. Y. MA, Y. ONO, L. STECKER, D. R. EVANS and S. T. HSU, *Tech. Dig. Int. Electron Devices Meet.* **149** (1999).
12. R. THERRIEN, B. RAYNER and G. LUCOVSKY, in Proceedings of the 4th International Symposium on the Physics and Chemistry of SiO$_2$ and the Si–SiO$_2$ Interface, 2000, p. 495.
13. M. BALOG, M. SCHIEBER, M. MICHMAN and S. PATAI, *Thin Solid Films* **47** (1977) 109.
14. J. SHAPPIR, A. ANIS and I. PINSKY, *IEEE Trans. Electron Devices* **ED-33** (1986) 442.
15. Y.-M. GAO, P. WU, R. KERSHAW, K. DWIGHT and A. WOLD, *Mat. Res. Bull.* **25** (1990) 871.
16. J. C. VIGUIE and J. SPITZ, *J. Electrochem. Soc.* **122** (1975) 585.
17. M. LANGLET and J. C. JOUBERT, in ''Chemistry of Advanced Materials'' (Blackwell Science, Oxford, England, 1993) p. 55.
18. CRC Handbook of Chemistry and Physics, CRC Press, Boca Raton, FL, 1984.
19. H. C. ZENG and S. SHI, *J. Non-Crys. Solids* **185** (1995) 31.
20. G. E. JELLISON JR., *J. Appl. Phys.* **69** (1991) 7627.
21. W. KERN and V. S. BAN, in ''Thin Film Process'' (Academic Press, Inc., 1978) p. 258.
22. T. MARUYAMA and S. ARAI, *Appl. Phys. Lett.* **60** (1992) 322.
23. W. A. PLISKIN and S. H. LEHMAN, *J. Electrochem. Soc.* **112** (1965) 1013.
24. R. AYOUCHI, F. MARTIN, D. LEINEN and J. R. RAMOS-BARRADO, *J. Crys. Growth* **247** (2003) 497.
25. G. D. WILK, R. M. WALLACE and J. M. ANTHONY, *J. Appl. Phys.* **89** (2001) 5243.